

Accuracy of Kohn-Sham density functional theory for warm- and hot-dense matter equation of state

Phanish Suryanarayana,^{1,*} Arpit Bhardwaj,¹ Xin Jing,¹ and John E. Pask²

¹*College of Engineering, Georgia Institute of Technology, Atlanta, Georgia 30332, USA*

²*Physics Division, Lawrence Livermore National Laboratory, Livermore, California 94550, USA*

(Dated: August 17, 2023)

We study the accuracy of Kohn-Sham density functional theory (DFT) for warm- and hot-dense matter (WDM and HDM). Specifically, considering a wide range of systems, we perform accurate ab initio molecular dynamics simulations with temperature-independent local/semilocal density functionals to determine the equations of state at compression ratios of 3x–7x and temperatures near 1 MK. We find very good agreement with path integral Monte Carlo (PIMC) benchmarks, while having significantly smaller error bars and smoother data, demonstrating the fidelity of DFT for the study of WDM and HDM.

I. INTRODUCTION

Warm- and hot-dense matter (WDM and HDM) arise in diverse physical systems such as the interiors of stars and giant planets as well as inertial confinement fusion (ICF) and other high energy density (HED) experiments [1]. The ability to accurately model WDM and HDM is therefore a key component in the understanding and design of ICF experiments as well as understanding the formation, nature, and evolution of planetary/stellar systems. However, such extreme conditions of temperature and pressure pose a significant challenge both experimentally and theoretically since both classical and quantum mechanical (degeneracy) effects occur, with the relative dominance of each varying with density and temperature.

Path integral Monte Carlo (PIMC) is a many-body method for the study of materials systems from the first principles of quantum mechanics, without any empirical or adjustable parameters [2]. Though highly accurate and capable of producing benchmark results, the PIMC method has significant computational cost. This cost, however, decreases with increase in temperature, allowing for the study of systems at temperatures associated with WDM/HDM [3–25]. However, despite significant advances, PIMC calculations remain limited in practice to small systems of low-Z elements at temperatures at or above the upper (lower) end of WDM (HDM) conditions. Furthermore, quantities of interest such as ionic transport properties are not accessible.

Kohn-Sham density functional theory (DFT) [26–28] is among the most widely used first principles methods for the study of materials systems. Given its high accuracy-to-cost ratio relative to other ab initio methods such as PIMC, DFT has become a cornerstone of modern materials science research, particularly for systems at or near ambient conditions [29]. However, Kohn-Sham calculations scale cubically with the number of states computed [30], making calculations at high temperature particularly expensive given the increase in partially occupied

states with temperature. This bottleneck is particularly acute in ab initio molecular dynamics (AIMD) simulations, where the Kohn-Sham equations may need to be solved thousands or hundreds of thousands of times to reach time scales of interest [29]. Consequently, conventional cubic-scaling Kohn-Sham DFT has found rather limited use in the study of WDM and HDM [3–10, 14–25, 31, 32]. This has motivated the development of new solution strategies to increase the efficiency of Kohn-Sham calculations under such conditions [33–41]. However, despite significant advances, the accuracy of Kohn-Sham DFT for WDM and HDM has not been clearly and comprehensively assessed heretofore.

In this work, we quantify the accuracy of Kohn-Sham DFT for WDM and HDM by carrying out a comprehensive comparison of highly accurate Kohn-Sham results to available PIMC benchmarks [25]. In particular, we employ the linear scaling Spectral Quadrature (SQ) method [33, 34, 42] implemented in the open-source SPARC electronic structure code [43–45] to perform AIMD simulations to determine the equations of state at compression ratios of 3x–7x and temperatures near 1 MK for a wide range of systems in the FPEOS database [25]. The SQ method enables systematic convergence of full Kohn-Sham energies, forces, and stresses to high accuracy at WDM/HDM conditions [33–35], without homogeneous electron gas (HEG) approximations [37, 38, 41] or large prefactors to reduce statistical errors in pressure to 0.05% [39, 40].

II. SPECTRAL QUADRATURE DENSITY FUNCTIONAL THEORY

Neglecting spin and Brillouin zone integration, the single-particle finite-temperature density matrix in Kohn-Sham DFT [26–28] can be written as

$$\mathcal{D} = f(\mathcal{H}) = \left(1 + \exp \left(\frac{\mathcal{H} - \mu\mathcal{I}}{k_B T} \right) \right)^{-1}, \quad (1)$$

where f is the Fermi-Dirac function, \mathcal{H} is the Hamiltonian matrix, \mathcal{I} is the identity matrix, k_B is the Boltz-

* phanish.suryanarayana@ce.gatech.edu

mann constant, T is the temperature, and μ is the Fermi level, obtained by enforcing the constraint on the total number of electrons. The calculation of the density matrix represents a nonlinear problem since the Hamiltonian itself depends on the components of the density matrix. Once the self-consistent solution has been obtained, the ground state density matrix can be used to compute quantities of interest such as the free energy, Hellmann-Feynman atomic forces, and Hellmann-Feynman stress tensor.

The finite-temperature density matrix has exponential decay away from its diagonal within a real-space representation [46–49], a consequence of the locality of electronic interactions, commonly referred to as “nearsightedness” in many-atom systems [50]. This decay can be exploited in the development of reduced scaling solution methods for the Kohn-Sham problem [51, 52]. One such linear scaling method that is particularly well suited to calculations at high temperature is referred to as Spectral Quadrature (SQ) [42]. In the SQ method, the decay in the density matrix is exploited to approximate quantities of interest, such as density, energy, and forces, as spatially localized bilinear forms or sums of bilinear forms, which are then approximated by quadrature rules. For instance, within a real-space finite-difference representation, the diagonal of the density matrix is the electron density, whose value at the n -th finite-difference node can be approximated as

$$e_n^T \mathcal{D} e_n \approx \sum_{k=1}^{N_q} w_{n,k} f(\lambda_{n,k}), \quad (2)$$

where e_n is the standard basis vector, N_q is the quadrature order, $\lambda_{n,k}$ are the quadrature nodes, and $w_{n,k}$ are the corresponding quadrature weights. The weights can be formally written as

$$w_{n,k} = e_s^T L_k(\mathcal{H}_n) e_s, \quad (3)$$

where L_k are the Lagrange polynomials, and e_s is the standard basis vector associated with the n -th finite-difference node subsequent to forming the truncated Hamiltonian \mathcal{H}_n for that node. In practice, the quadrature weights are not evaluated using Eq. 3 directly since the computational cost would scale quadratically with quadrature order. Rather, the weights are evaluated using alternate polynomial bases whose product with the vector e_s can be evaluated using efficient three-term recurrence relations, whereby the computational cost scales linearly with the quadrature order. In so doing, off-diagonal components of the truncated density matrix also become available, which can be used to efficiently calculate quantities such as atomic forces and stress tensor.

In the absence of truncation, the Gauss and Clenshaw-Curtis variants of the SQ method reduce to the recursion [53, 54] and classical Fermi operator expansion (FOE) [55, 56] methods, respectively. The SQ method is applicable to metallic and insulating systems alike, with increasing efficiency at higher temperature as the density

matrix becomes more localized and the Fermi operator becomes smoother [33, 34, 49]. On increasing quadrature order and localization radius, the exact diagonalization limit can be obtained to desired accuracy, with convergence to standard $O(N^3)$ planewave results readily obtained for metallic and insulating systems alike [33–35]. The SQ method also provides results for the infinite-crystal without recourse to Brillouin zone integration or large supercells [33, 34, 57], a technique referred to as the infinite-cell method.

III. RESULTS AND DISCUSSION

We now verify the accuracy of Kohn-Sham DFT for the study of WDM and HDM. To do so, we consider the following systems at compression ratios of 3x–7x and temperatures near 1 MK: hydrogen (H), helium (He), boron (B), carbon (C), nitrogen (N), oxygen (O), neon (Ne), magnesium (Mg), lithium fluoride (LiF), boron nitride (BN), hydrocarbon (CH), boron carbide (B_4C), and magnesium silicate ($MgSiO_3$). These form a representative set of systems from the first-principles equation of state (FPEOS) database [25] for which PIMC data is available, providing a stringent test of DFT’s accuracy.

To determine the pressure and internal energy at a given density and temperature, we perform isokinetic ensemble (NVK) AIMD simulations with a Gaussian thermostat [58]. We consider 32-atom cells for all systems other than B_4C and $MgSiO_3$, for which we consider 40-atom cells. We employ the temperature-independent local density approximation (LDA) as the exchange-correlation functional [26, 59]. To assess the effect of the exchange-correlation functional, we also consider the temperature-independent semilocal Perdew–Burke–Ernzerhof (PBE) [60] exchange-correlation functional for H, BN, and $MgSiO_3$. We employ optimized norm conserving Vanderbilt (ONCV) pseudopotentials [61] with 1, 2, 5, 6, 7, 8, 10, 10, 3, 9, and 12 electrons in valence for H, He, B, C, N, O, Ne, Mg, Li, F, and Si, respectively. These pseudopotentials, most of which are all-electron, have been constructed for target accuracy at the conditions considered.

We perform all calculations using the recently developed implementation of SQ in the open-source SPARC electronic structure code [43–45]. In particular, Gauss SQ is used for calculation of the electron density and energy [33, 34, 42], whereas Clenshaw-Curtis SQ is used for calculation of the forces and the pressure [33–35]. Numerical parameters in the SQ DFT calculation (grid spacing, quadrature order, and localization radius) are chosen to converge pressures to 0.5 % or less (discretization error). A time step of 0.04 fs is used in AIMD simulations, where the initial ~ 500 steps are used for equilibration and the following ~ 8000 steps are used for production, which reduces error bars on the pressure to 0.05% or less (statistical error).

The results so obtained are presented in Table I, from

TABLE I: Pressure and internal energy as computed by DFT (LDA) and PIMC [25]. The number in brackets represents the DFT result for the PBE exchange-correlation functional.

Material	Density (g/cm ³)	Comp. ratio	Temperature (K)	Pressure (GPa)		Internal energy (Ha/fu)	
				DFT	PIMC	DFT	PIMC
H	0.25	2.961	1 000 000	4 082 ± 1.8 (4 080 ± 1.5)	4 094 ± 3	0.071 ± 0.008 (0.067 ± 0.002)	0.078 ± 0.007
H	0.42	4.901	1 000 000	6 730 ± 1.1 (6 730 ± 1.7)	6 744 ± 6	-0.016 ± 0.003 (-0.015 ± 0.002)	-0.017 ± 0.008
H	0.50	5.884	1 000 000	8 068 ± 1.8 (8 069 ± 2.2)	8 080 ± 7	-0.055 ± 0.004 (-0.052 ± 0.001)	-0.061 ± 0.009
He	0.39	3.135	1 000 000	2 297 ± 0.8	2 308 ± 1	0.166 ± 0.009	0.173 ± 0.004
He	0.50	4.071	1 000 000	2 965 ± 0.9	2 981 ± 1	0.003 ± 0.009	0.013 ± 0.003
He	0.67	5.418	1 000 000	3 930 ± 0.9	3 941 ± 1	-0.169 ± 0.005	-0.186 ± 0.003
B	7.40	3.000	1 010 479	24 839 ± 8	24 394 ± 259	1.065 ± 0.005	1.089 ± 0.217
B	9.86	4.000	1 010 479	33 306 ± 13	32 938 ± 370	0.172 ± 0.005	0.357 ± 0.232
B	11.09	4.500	1 010 479	37 671 ± 18	36 229 ± 419	-0.115 ± 0.007	-0.496 ± 0.233
B	12.33	5.000	1 010 479	42 131 ± 20	41 519 ± 466	-0.359 ± 0.007	-0.250 ± 0.234
B	14.79	6.000	1 010 479	51 069 ± 25	50 185 ± 602	-0.763 ± 0.007	-0.700 ± 0.251
C	8.50	2.415	1 010 479	28 266 ± 12	28 519 ± 32	0.836 ± 0.007	0.908 ± 0.016
C	10.33	2.938	1 010 479	34 666 ± 16	35 049 ± 40	0.325 ± 0.009	0.369 ± 0.018
C	12.64	3.590	1 010 479	42 942 ± 20	43 579 ± 52	-0.110 ± 0.009	-0.088 ± 0.018
C	15.50	4.407	1 010 479	53 739 ± 24	54 665 ± 57	-0.413 ± 0.010	-0.456 ± 0.016
C	19.37	5.509	1 010 479	68 910 ± 34	70 512 ± 102	-0.638 ± 0.011	-0.733 ± 0.023
N	2.53	3.129	998 004	7 767 ± 3	7 727 ± 9	0.759 ± 0.010	1.631 ± 0.051
N	3.71	4.588	998 004	11 333 ± 4	11 155 ± 21	-0.759 ± 0.009	-1.631 ± 0.060
O	2.49	3.727	998 004	7 328 ± 3	7 337 ± 10	0.763 ± 0.009	0.747 ± 0.040
O	3.63	5.442	998 004	10 626 ± 5	10 570 ± 14	-0.763 ± 0.010	-0.747 ± 0.042
Ne	3.73	2.473	998 004	9 956 ± 4	9 896 ± 20	2.223 ± 0.007	2.166 ± 0.084
Ne	7.90	5.239	998 004	20 931 ± 10	20 731 ± 46	-2.223 ± 0.007	-2.166 ± 0.073
Mg	4.31	2.478	1 010 479	10 455 ± 4	10 695 ± 300	-16.171 ± 0.008	-146.075 ± 0.965
LiF	7.58	2.877	998 004	22 955 ± 10	22 573 ± 25	1.757 ± 0.014	1.127 ± 0.049
LiF	15.70	5.958	998 004	49 009 ± 23	48 415 ± 42	-1.757 ± 0.018	-1.127 ± 0.039
BN	6.77	3.000	1 010 479	21 813 ± 9 (21 803 ± 7)	21 447 ± 629	2.057 ± 0.014 (2.007 ± 0.008)	1.482 ± 1.317
BN	9.03	4.000	1 010 479	29 295 ± 13 (29 361 ± 13)	28 664 ± 775	0.366 ± 0.018 (0.395 ± 0.018)	-0.269 ± 1.217
BN	10.16	4.500	1 010 479	33 052 ± 15 (33 183 ± 15)	32 070 ± 861	-0.234 ± 0.012 (-0.218 ± 0.016)	-1.419 ± 1.201
BN	11.29	5.000	1 010 479	37 019 ± 17 (37 048 ± 17)	36 758 ± 462	-0.707 ± 0.020 (-0.744 ± 0.016)	-0.456 ± 1.201
BN	13.55	6.000	1 010 479	44 949 ± 22 (45 124 ± 20)	46 719 ± 1087	-1.482 ± 0.020 (-1.440 ± 0.020)	0.664 ± 1.138
CH	3.15	3.000	1 347 305	19 355 ± 8	19 198 ± 326	2.541 ± 0.018	1.822 ± 0.770
CH	4.20	4.000	1 347 305	25 616 ± 10	26 274 ± 394	0.557 ± 0.016	1.563 ± 0.700
CH	4.72	4.500	1 347 305	28 728 ± 12	28 857 ± 445	-0.213 ± 0.014	-0.243 ± 0.701
CH	5.25	5.000	1 347 305	31 860 ± 14	33 015 ± 500	-0.875 ± 0.012	0.444 ± 0.710
CH	6.30	6.000	1 347 305	38 123 ± 10	37 343 ± 572	-2.010 ± 0.012	-3.586 ± 0.675
B ₄ C	7.53	3.000	1 010 479	25 208 ± 10	24 093 ± 676	5.686 ± 0.030	-1.656 ± 2.836
B ₄ C	10.03	4.000	1 010 479	33 893 ± 15	34 986 ± 1044	1.511 ± 0.040	2.301 ± 3.285
B ₄ C	11.29	4.500	1 010 479	38 275 ± 19	41 709 ± 1143	-0.134 ± 0.045	7.075 ± 3.197
B ₄ C	15.05	6.000	1 010 479	52 141 ± 23	53 347 ± 1466	-2.944 ± 0.040	-2.840 ± 3.077
B ₄ C	17.56	7.000	1 010 479	61 691 ± 30	62 336 ± 1580	-4.119 ± 0.045	-4.880 ± 2.836
MgSiO ₃	9.62	3.000	1 347 305	36 342 ± 17 (36 422 ± 18)	37 637 ± 486	12.262 ± 0.060 (12.253 ± 0.050)	12.518 ± 2.892
MgSiO ₃	12.83	4.000	1 347 305	48 687 ± 19 (48 770 ± 18)	49 919 ± 632	2.387 ± 0.065 (2.345 ± 0.060)	-0.508 ± 2.821
MgSiO ₃	14.44	4.500	1 347 305	54 993 ± 19 (55 125 ± 26)	57 845 ± 716	-1.298 ± 0.050 (-1.176 ± 0.045)	2.085 ± 2.838
MgSiO ₃	16.04	5.000	1 347 305	61 481 ± 22 (61 488 ± 26)	62 594 ± 792	-4.153 ± 0.080 (-4.372 ± 0.065)	-7.665 ± 2.830
MgSiO ₃	19.25	6.000	1 347 305	74 466 ± 35 (74 631 ± 27)	78 261 ± 967	-9.198 ± 0.065 (-9.050 ± 0.060)	-6.429 ± 2.877

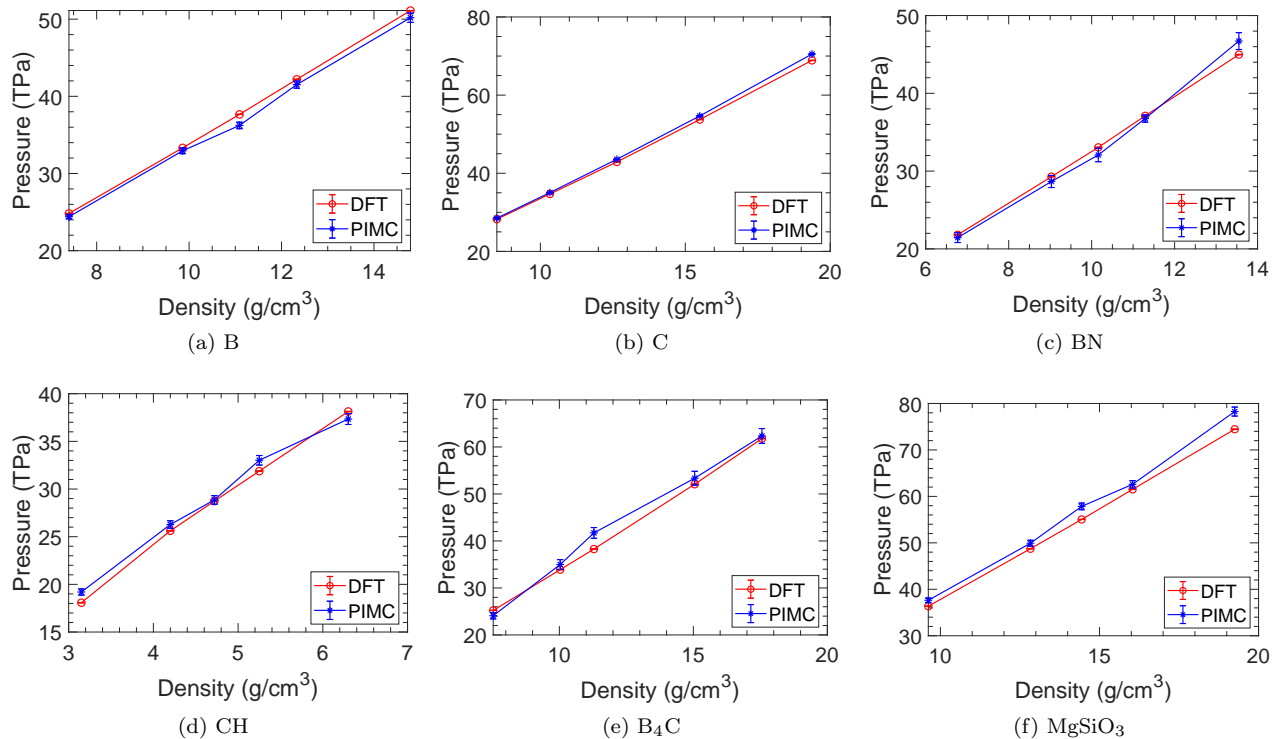


FIG. 1: Variation of pressure with density for DFT (LDA) and PIMC [25].

which we make the following observations. First, there is excellent agreement between the DFT results here and those in recent work for BN [6], confirming the accuracy of the simulations. Second, there is excellent agreement between the LDA and PBE results, with root mean square differences in pressure and internal energy of 0.2% and 0.085 Ha/fu, respectively. This shows that DFT results are insensitive, to this accuracy, to the choice of exchange-correlation functional at these conditions, for functionals constructed to be exact in the limit of the HEG in particular. This is consistent with previous findings for comparably well converged Kohn-Sham calculations of BN [6] and C [62] at such conditions. Third, there is very good agreement between DFT and PIMC in the pressure, with a root mean square difference of $\sim 2.5\%$, the larger differences occurring for systems with larger PIMC error bars. This level of agreement is notable given the fundamental differences between the two first principles methods; e.g., while PIMC calculations typically employ the fixed node approximation, they are free of the Born-Oppenheimer, exchange-correlation, and pseudopotential approximations in the DFT calculations. This demonstrates the accuracy of DFT for the study of WDM and HDM using standard temperature-independent local/semilocal exchange-correlation functionals constructed to be exact in the HEG limit. Note that the internal energy computed in DFT and PIMC is also found to be in good agreement. Fourth, the error bars in DFT are noticeably tighter than PIMC, with

root mean square pressure error bar of 0.04% and 1.5% for DFT and PIMC, respectively. This translates to significantly smoother variation in the DFT results, as evident from Fig. 1, where the pressure has been plotted as a function of density for B, C, BN, CH, B₄C, and MgSiO₃. In particular, the DFT pressure is found to vary linearly with density, in agreement with the overall trend displayed by the PIMC pressure, which is otherwise more jagged. Taken as a whole, the results demonstrate excellent agreement between well-converged DFT-LDA/GGA and PIMC ab initio results for a wide range of WDM/HDM systems despite the different approximations employed in each.

IV. CONCLUDING REMARKS

In this work, we have demonstrated the accuracy of Kohn-Sham DFT for WDM and HDM. Specifically, using the state-of-the-art SQ method, we have performed accurate AIMD simulations with temperature-independent local/semilocal density functionals to determine the equations of state for a wide range of systems at compression ratios of 3x–7x and temperatures around 1 MK. In particular, we have found excellent agreement with PIMC benchmarks, with the DFT data being smoother and having significantly smaller error bars, demonstrating the accuracy of DFT at the conditions of temperature and pressure associated with WDM/HDM.

The current work further highlights the importance of developing new methods for the efficient solution of the Kohn-Sham equations at high temperature, making it a worthy subject of research.

ACKNOWLEDGEMENTS

P.S. and X.J. gratefully acknowledge support from grant DE-NA0004128 funded by the U.S. Department of Energy (DOE), National Nuclear Security Administration (NNSA). J.E.P gratefully acknowledges support from the U.S. DOE, NNSA: Advanced Simulation and Computing (ASC) Program at Lawrence Livermore National Laboratory (LLNL). This work was performed in part under the auspices of the U.S. DOE by LLNL under Contract DE-AC52-07NA27344.

-
- [1] F. Graziani, M. P. Desjarlais, R. Redmer, and S. B. Trickey, eds., *Frontiers and Challenges in Warm Dense Matter*, Lecture Notes in Computational Science and Engineering (Springer, 2014).
 - [2] J. A. Barker, *The Journal of Chemical Physics* **70**, 2914 (1979).
 - [3] K. P. Driver, F. Soubiran, and B. Militzer, *Physical Review E* **97**, 063207 (2018).
 - [4] S. Zhang, B. Militzer, M. C. Gregor, K. Caspersen, L. H. Yang, J. Gaffney, T. Ogitsu, D. Swift, A. Lazicki, D. Erskine, *et al.*, *Physical Review E* **98**, 023205 (2018).
 - [5] S. Zhang, M. C. Marshall, L. H. Yang, P. A. Sterne, B. Militzer, M. Däne, J. A. Gaffney, A. Shamp, T. Ogitsu, K. Caspersen, *et al.*, *Physical Review E* **102**, 053203 (2020).
 - [6] S. Zhang, A. Lazicki, B. Militzer, L. H. Yang, K. Caspersen, J. A. Gaffney, M. W. Däne, J. E. Pask, W. R. Johnson, A. Sharma, *et al.*, *Physical Review B* **99**, 165103 (2019).
 - [7] K. P. Driver and B. Militzer, *Physical Review Letters* **108**, 115502 (2012).
 - [8] L. X. Benedict, K. P. Driver, S. Hamel, B. Militzer, T. Qi, A. A. Correa, A. Saul, and E. Schwegler, *Physical Review B* **89**, 224109 (2014).
 - [9] S. Zhang, B. Militzer, L. X. Benedict, F. Soubiran, P. A. Sterne, and K. P. Driver, *The Journal of Chemical Physics* **148**, 102318 (2018).
 - [10] S. Zhang, K. P. Driver, F. Soubiran, and B. Militzer, *Physical Review E* **96**, 013204 (2017).
 - [11] B. Militzer and D. M. Ceperley, *Physical Review E* **63**, 066404 (2001).
 - [12] S. X. Hu, B. Militzer, V. N. Goncharov, S. Skupsky, *et al.*, *Physical Review B* **84**, 224109 (2011).
 - [13] B. Militzer, W. Magro, and D. Ceperley, *Contributions to Plasma Physics* **39**, 151 (1999).
 - [14] B. Militzer, *Physical Review B* **79**, 155105 (2009).
 - [15] B. Militzer, *Physical Review Letters* **97**, 175501 (2006).
 - [16] K. P. Driver and B. Militzer, *Physical Review E* **95**, 043205 (2017).
 - [17] F. González-Cataldo, F. Soubiran, and B. Militzer, *Physics of Plasmas* **27**, 092706 (2020).
 - [18] F. Soubiran, F. González-Cataldo, K. P. Driver, S. Zhang, and B. Militzer, *The Journal of Chemical Physics* **151**, 214104 (2019).
 - [19] F. González-Cataldo, F. Soubiran, H. Peterson, and B. Militzer, *Physical Review B* **101**, 024107 (2020).
 - [20] K. P. Driver and B. Militzer, *Physical Review B* **93**, 064101 (2016).
 - [21] S. Zhang, K. P. Driver, F. Soubiran, and B. Militzer, *The Journal of Chemical Physics* **146**, 074505 (2017).
 - [22] K. P. Driver and B. Militzer, *Physical Review B* **91**, 045103 (2015).
 - [23] K. P. Driver, F. Soubiran, S. Zhang, and B. Militzer, *The Journal of Chemical Physics* **143**, 164507 (2015).
 - [24] B. Militzer and K. P. Driver, *Physical Review Letters* **115**, 176403 (2015).
 - [25] B. Militzer, F. González-Cataldo, S. Zhang, K. P. Driver, and F. Soubiran, *Physical Review E* **103**, 013203 (2021).
 - [26] W. Kohn and L. J. Sham, *Physical Review* **140**, A1133 (1965).
 - [27] P. Hohenberg and W. Kohn, *Physical Review* **136**, B864 (1964).
 - [28] N. D. Mermin, *Physical Review* **137**, A1441 (1965).
 - [29] K. Burke, *The Journal of chemical physics* **136**, 150901 (2012).
 - [30] R. M. Martin, *Electronic structure: basic theory and practical methods* (Cambridge university press, 2020).
 - [31] M. Bethkenhagen, A. Sharma, P. Suryanarayana, J. E. Pask, B. Sadigh, and S. Hamel, *Physical Review E* **107**, 015306 (2023).
 - [32] C. J. Wu, P. C. Myint, J. E. Pask, C. J. Prisbrey, A. A. Correa, P. Suryanarayana, and J. B. Varley, *The Journal of Physical Chemistry A* **125**, 1610 (2021).
 - [33] P. P. Pratapa, P. Suryanarayana, and J. E. Pask, *Computer Physics Communications* **200**, 96 (2016).
 - [34] P. Suryanarayana, P. P. Pratapa, A. Sharma, and J. E. Pask, *Computer Physics Communications* **224**, 288 (2018).
 - [35] A. Sharma, S. Hamel, M. Bethkenhagen, J. E. Pask, and P. Suryanarayana, *The Journal of Chemical Physics* **153**, 034112 (2020).
 - [36] Q. Xu, X. Jing, B. Zhang, J. E. Pask, and P. Suryanarayana, *The Journal of Chemical Physics* **156**, 094105 (2022).
 - [37] S. Zhang, H. Wang, W. Kang, P. Zhang, and X. T. He, *Physics of Plasmas* **23**, 042707 (2016).
 - [38] A. Blanchet, J. Clérouin, M. Torrent, and F. Soubiran, *Computer Physics Communications* , 108215 (2021).
 - [39] Y. Cytter, E. Rabani, D. Neuhauser, and R. Baer, *Physical Review B* **97**, 115207 (2018).
 - [40] A. J. White and L. A. Collins, *Physical Review Letters* **125**, 055002 (2020).

- [41] B. Sadigh, D. Aberg, and J. Pask, arXiv preprint arXiv:2305.08762 (2023).
- [42] P. Suryanarayana, Chemical Physics Letters **584**, 182 (2013).
- [43] Q. Xu, A. Sharma, B. Comer, H. Huang, E. Chow, A. J. Medford, J. E. Pask, and P. Suryanarayana, SoftwareX **15**, 100709 (2021).
- [44] B. Zhang, X. Jing, Q. Xu, S. Kumar, A. Sharma, L. Erlandson, S. J. Sahoo, E. Chow, A. J. Medford, J. E. Pask, *et al.*, arXiv preprint arXiv:2305.07679 (2023).
- [45] S. Ghosh and P. Suryanarayana, Computer Physics Communications **216**, 109 (2017).
- [46] S. Goedecker, Physical Review B **58**, 3501 (1998).
- [47] S. Ismail-Beigi and T. A. Arias, Physical Review Letters **82**, 2127 (1999).
- [48] M. Benzi, P. Boito, and N. Razouk, SIAM Review **55**, 3 (2013).
- [49] P. Suryanarayana, Chemical Physics Letters **679**, 146 (2017).
- [50] E. Prodan and W. Kohn, Proceedings of the National Academy of Sciences of the United States of America **102**, 11635 (2005).
- [51] D. R. Bowler, T. Miyazaki, and M. J. Gillan, Journal of Physics: Condensed Matter **14**, 2781 (2002).
- [52] S. Goedecker, Reviews of Modern Physics **71**, 1085 (1999).
- [53] Haydock, R and Heine, V and Kelly, M J, Journal of Physics C: Solid State Physics **5**, 2845 (1972).
- [54] R. Haydock, V. Heine, and M. J. Kelly, Journal of Physics C: Solid State Physics **8**, 2591 (1975).
- [55] S. Goedecker and L. C, Physical Review Letters **73**, 122 (1994).
- [56] S. Goedecker and M. Teter, Physical Review B **51**, 9455 (1995).
- [57] P. Suryanarayana, K. Bhattacharya, and M. Ortiz, Journal of the Mechanics and Physics of Solids **61**, 38 (2013).
- [58] P. Minary, G. J. Martyna, and M. E. Tuckerman, The Journal of chemical physics **118**, 2510 (2003).
- [59] J. P. Perdew and Y. Wang, Physical Review B **45**, 13244 (1992).
- [60] J. P. Perdew, K. Burke, and M. Ernzerhof, Physical Review Letters **77**, 3865 (1996).
- [61] D. R. Hamann, Physical Review B **88**, 085117 (2013).
- [62] M. Bonitz, T. Dornheim, A. Moldabekov, S. Zhang, P. Hamann, H. Kahlert, A. Filinov, K. Ramakrishna, and J. Vorberger, Phys. Plasmas **27**, 042710 (2020).